February 2002

# Experimental study of streamers in pure $N_2$ and $N_2/O_2$ mixtures and a ≈13 cm gap

Won J. Yi
*University of Nebraska - Lincoln*

P. F. Williams
*University of Nebraska - Lincoln*, pfw@moi.unl.edu

Published in *Journal of Physics D: Applied Physics* **35**:3 (February 7, 2002), pp. 205-218;
doi 10.1088/0022-3727/35/3/308 

Submitted October 11, 2001; published online January 22, 2002.

# Experimental study of streamers in pure $N_2$ and $N_2/O_2$ mixtures and a ≈13 cm gap

Won J. Yi and P. F. Williams

Department of Electrical Engineering, University of Nebraska–Lincoln,
Lincoln, NE 68588-0511, USA; Email: pfw@moi.unl.edu

**Abstract**
Empirical data on streamer formation and propagation in near-atmospheric pressure $N_2$ and $N_2/O_2$ mixtures are presented. The data were obtained primarily from high-speed, high-sensitivity shutter and streak photography of streamers produced in a ≈13 cm gap. The streamer propagation velocity as a function of applied voltage, polarity, total pressure, and $O_2$ concentration are provided. In addition, information on streamer bifurcation, and streamer shape and size is included.

The breakdown process has two phases: a fast phase featuring the propagation of streamers, and much slower phase involving the heating of the gas to form the spark channel. Also we found that the addition of $O_2$ significantly alters the streamer characteristics and behavior, indicating that photoionization processes play an important role.

## 1. Introduction

The electrical breakdown of gases has received a great deal of interest for many years [1]. It is now well accepted that electrical breakdown at around atmospheric pressures often proceeds via the creation and propagation of streamers. These are needle-shaped regions of free ionization embedded within relatively unionized gas that can grow even in average applied fields well below those required for significant electron impact ionization. Field enhancement at the sharp tip of streamers allows the creation of substantial free ionization even in low average fields.

In this paper, we report the results of a systematic study of streamers in $N_2$, and mixtures of $N_2$ with $O_2$ in a 13 cm gap. The primary diagnostics are high-speed, high-sensitivity streak and shutter photography. Several reports of measurements of streamer velocity have appeared; however, these reports are rather inconsistent. The inconsistency in many cases is probably due to the experimental design. With this in mind, we have designed our experiments to minimize the dependence of measured properties on uncontrolled parameters such as free-ionization density left by the initiating electron avalanche. Specifically, our experiments differ from those reported by other workers in two principal ways. First, the 13 cm gap length is intermediate between the 1–3 cm lengths typically used in controlled atmosphere laboratory experiments and the 1–10m lengths employed in open-air experiments. The gap is long enough to allow "steady-state" propagation to be achieved, but short enough to allow the use of a controlled environment. Second, streamers in our experiments are intentionally initiated very close to a small point projecting from the surface of one electrode, rather than from a diffuse electron avalanche which reaches the critical density for streamer formation somewhere in midgap. As discussed in section 4, our configuration decouples better streamer evolution from the initiating avalanche evolution, and should provide data more representative of the streamer properties. Additionally, the ≈20 ns voltage pulse risetime is unusually fast for such a large system. In comparison to systems with $\mu$s risetime, the fast risetime in our system reduces interpretational complications.

The breakdown process in our gap has two phases. One involves the propagation of streamers (fast phase), and the other the growth of one or more highly conductive filamentary channels (slow phase).

## 2. Experimental setup

Figure 1 shows a schematic diagram of the apparatus we used in this study. The test electrodes are enclosed in a vacuum-tight, 9 cm long, 56 cm diameter steel chamber. To obtain consistent experimental conditions, the experimental chamber was evacuated to 20mtorr and then backfilled with the desired test gas to a pressure up to 900 torr. The leak rate under vacuum was about 4 m torr $min^{-1}$. Three windows provide optical access to the gap region. Two of the windows view the gap region from opposite sides of the chamber along a horizontal axis perpendicular to the gap axis. The diameter of these windows is ≈15 cm. The third window (not shown in figure 1) has a diameter of about 2.5 cm, and views the gap region along a vertical axis. The gap separation is adjustable, but for all experiments discussed here the separation was 14.3 cm. The electrode diameter was about 15 cm. In most experiments a small, sharp point projected 1 cm into the gap from the centre of the charged electrode. The point was made of 1/8 inch (3.2 mm) steel drill rod ground to a sharp point on one end. The profile of the tip is not well known. The radius of curvature was less than 100$\mu$m, and the tapered region was about 0.5 cm long. A small "muffin" fan was placed in the bottom of the chamber to enhance uniformity of gas mixtures.

To provide the best electrical characteristics, the system was designed to be completely enclosed in a grounded outer conductor, in a coaxial geometry. The gap electrodes are connected to the outside world through electrical feedthroughs consisting of aluminium center conductors and Lexan insulators. Diameters were chosen to provide a roughly constant line impedance of 50 Ω. The uncharged electrode is grounded through a 50 Ω resistor made up of two Carborundum Corp. type 889HS 25 Ω resistors in series. It was enclosed by Plexiglas tubing of 1/4 inch (6.3 mm) wall thickness to avoid breakdown of the Carborundum resistor to ground.

Voltage pulses are applied to the gap by using a laser-triggered spark gap to connect a 6 m length of charged RG-220/U coaxial cable to the electrode. The gap separation for the switch is about 2.5 cm, and the gap is pressurized with $N_2$ to about 5 atm, absolute. By varying the fill pressure or the gap separation, the spark gap can be operated reliably with charging voltages between about 60 and 150 kV. After the closure of the laser-triggered gap, but before the breakdown of the experimental gap, the end of the transmission line is open. To damp the ringing resulting from the pulse reflecting back and forth between the two ends of the line, a 180 Ω resistor was placed in series with the line. The resistor slowed the risetime of the pulse to about 20 ns, but damped the ringing substantially. A 250 MΩ resistor was used to drain charge from the line in case the experimental gap did not breakdown.

The voltage waveform applied to the gap for a 120 kV charge is shown in figure 2. In most of our experiments, streamers were initiated at 30–50 ns on this timescale, and required 300–400 ns to traverse the gap. During this time the voltage rings about an average value of about 98 kV. The reason for the difference between the initial charging voltage and the final voltage is primarily charge sharing between the capacitances of the initially charged line and the initially uncharged line and gap. Losses in the 180 Ω resistor and in the spark-gap-switch may also play a small role. Because of this ringing, the determination of streamer properties as a function of applied voltage is a bit ambiguous. In this paper, we have chosen to report voltage as the average voltage during this time. The initial charging voltage is 20% larger than this value.

The primary electrical diagnostics were three capacitively coupled voltage probes located as shown in figure 1. The probes measured the voltage on both sides of the 180 Ω damping resistor, and on the uncharged electrode. When used with a Tektronix 7834 storage oscilloscope and either Tektronix P6063B or P6009 probes, the overall risetime was less than 2 ns, and the drop time was about 3 ms. The gap current was inferred from the output of P3, under the assumption that the 50 Ω load was purely resistive.

Optical diagnostics centred on a streak camera and a shutter camera. The input optical systems were about *f*/4 and *f*/6 for the streak and shutter cameras, respectively. The photo-cathodes of both cameras have about 10% quantum efficiency in the visible and near ultraviolet. Transmission characteristics of the optical systems and the photo-cathode spectral response limited the useful spectral range to about

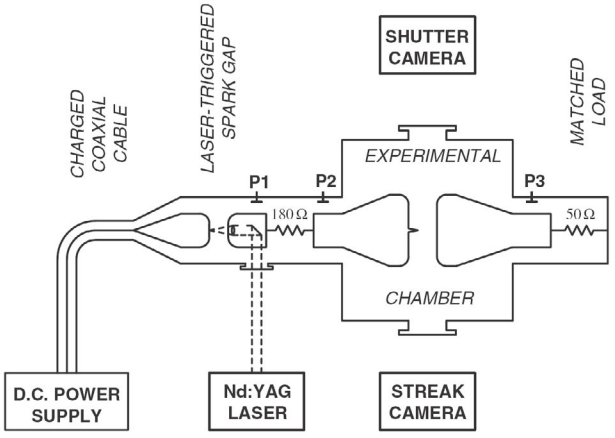


**Figure 1.** Schematic diagram of the experimental setup. P1, P2, and P3 are capacitively coupled voltage probes.

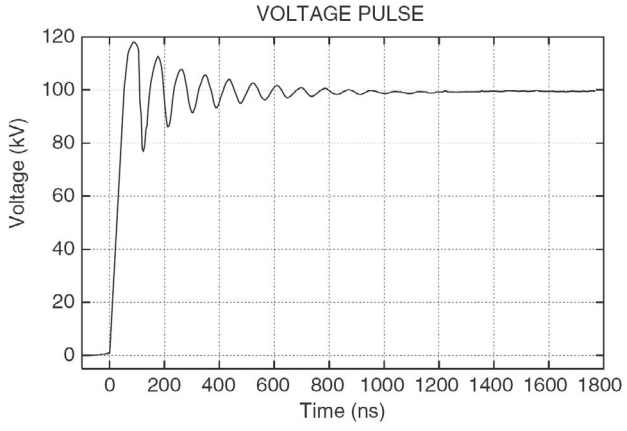


**Figure 2.** Oscillogram of a typical voltage pulse applied to the experimental chamber. The charging voltage was 120 kV, and the average gap voltage was 98 kV.

340–700 nm. The streak camera was a Hamamatsu C979 temporal disperser, coupled to a C1000-18 SIT vidicon camera with digital image storage. The system provided about 2 ns temporal resolution, with near-single-photon sensitivity. The shutter camera was locally constructed, and was based on an ITT F-4144 dual micro-channel plate image intensifier, specially modified for fast gating. The shutter time in all experiments reported here was about 10 ns.

The timing jitter in the delay to streamer initiation caused difficulty in all our experiments, but it was especially acute in the case of cathode-directed streamers in $O_2$-containing fill gas mixtures. To reduce this delay and jitter, an Hg spectral calibration lamp was used to irradiate the gap region. The intensity and spectral characterization of the irradiation is unknown, but a principal component was at 235 nm, and the intensity in the gap was probably between 10 and 100 mW $cm^{-2}$.

## 3. Experimental results

We have obtained shutter and streak photographs of streamers initiated at the tip of the sharp point projecting from one electrode, and propagating across an otherwise constant-field ≈13 cm gap. We have data for both polarities of the tip, for a range of charging voltages corresponding to average fields (charging voltage divided by electrode separation) ranging from about 6 to 10 kV $cm^{-1}$, for pure $N_2$ and mixtures of $N_2$ with $O_2$ and for a range of pressures ranging from 100 to 800 torr. The shutter photographs provide information about the spatial behavior of the streamers, while the streak photographs provide information about the temporal characteristics.

Data for both polarities of applied voltage to the tip were obtained. We call the streamers produced "cathode directed" for positive voltage applied to the tip and "anode directed" for negative voltage applied to the tip.

### *3.1. Shutter and streak photographs*

*3.1.1. Streamers in pure* $N_2$. Figure 3 shows a sequence of shutter photographs obtained in a pure $N_2$-filled gap. The point was positively charged so that these are photographs of cathode-directed streamers. Other conditions are given in the figure caption. Our camera can take only one photo per shot, so each picture is from a different shot. There was considerable shot-to-shot variation. Typically, the jitter in the initiation time was about 10 ns. The photos were selected to be representative of the typical evolution we observed. The multiple points of light are the luminous tips of streamers. The tips are elongated by motional blurring resulting from the combined effects of the 10 ns shutter time and the ≈10 ns radiative lifetime of the excited states producing the fluorescence. In figure 3(*d*), the lead streamers had already bridged the gap, and this and the following photographs show the heating of the detritus left behind.

It is evident that a large number of streamers are created under these conditions. It appears that several streamers are created at or near the tip, and that these streamers bifurcate frequently as they transit the gap, in a kind of chain reaction. About 370 ns was required for the lead streamer to reach the opposite electrode. From this point the streamers slowly developed into a high-conductivity filamentary channel, as shown in figures 3(*d*)–(*h*). This stage is similar to the leader formation stage of long gap breakdown. The time for the conductive filament to bridge the gap (2000–3000 ns) is much longer than the streamer propagation (300–400 ns) across the gap. Thus, the electrical breakdown in the gap occurs in two phases: a fast phase in which the streamers propagate, and a slow phase in which the highly conductive filamentary channels grow.

Figure 4 shows a sequence of shutter photographs obtained under similar conditions except that the charging polarity was reversed so that these are anode-directed streamers, and the charging voltage is 123 kV. As with the cathode-directed streamers, several streamers are initiated at or near the tip. The diameter of the body of these streamers appears to be somewhat larger, and the frequency of bifurcation smaller, than for the cathode-directed streamers. The luminous features associated with the streamer tips are longer in the anode-directed case as well. This lengthening may be due to greater motional blurring. The anode-directed streamers in figure 4 propagated about four times faster than did the cathode-directed streamers in figure 3.

An interesting feature of the anode-directed streamers is that for a pure $N_2$, 760 torr fill the streamers did not cross the entire gap at any applied voltage we investigated (up to 123 kV applied, 150 kV charging). Instead, they seemed to stop, and fade away at some midgap point. This feature is shown more clearly in the streak photographs presented in figure 5, which shows streak photographs of streamers of both polarities under otherwise similar conditions. Each photo shows a front propagating across the gap corresponding to the leading edge of the cloud of streamers. The front associated with the cathode-directed streamers starts with a speed of about $3 \times 10^8$ cm $s^{-1}$, and slows to constant speed of about $4 \times 10^7$ cm $s^{-1}$. The anode-directed streamer front, on the other hand, starts similarly and appears to slow to a speed of about $7 \times 10^7$ cm $s^{-1}$, and then fades and disappears about halfway across the gap.

*3.1.2. Streamers in* $N_2/O_2$ *mixtures.* The addition of small amounts of $O_2$ changes streamer characteristics substantially. Figure 6 shows shutter photographs of cathode-directed [(*a*) and (*c*)] and anode-directed [(*b*) and (*d*)] streamers in pure $N_2$ [(*a*) and (*b*)] and $N_2/O_2$ mixtures [(*c*) and (*d*)].

The addition of $O_2$ decreases the number of streamers, increases the diameter of the streamer body, and increases the apparent length of the streamer tip. Streak photographs show that the addition of $O_2$ increases streamer speed, and this increase in apparent length is consistent with motional blurring. The addition of $O_2$ reduces both the number of streamers produced near the tip, and the rate of bifurcation of these streamers in midgap.

Another consequence of $O_2$ addition with the cathode-directed polarity is a substantial increase in delay and jitter of the streamer initiation. With pure $N_2$, the time between the voltage rise and streamer initiation was typically 40 ns, with about ±10 ns jitter. Adding $O_2$ increased the delay to the 1$\mu$s range, with jitter comparable to the delay. We believe this behavior is due to the electron attachment properties of $O_2$ [2]. We found that irradiating the gap with light from an Hg vapor spectral calibration lamp reduced

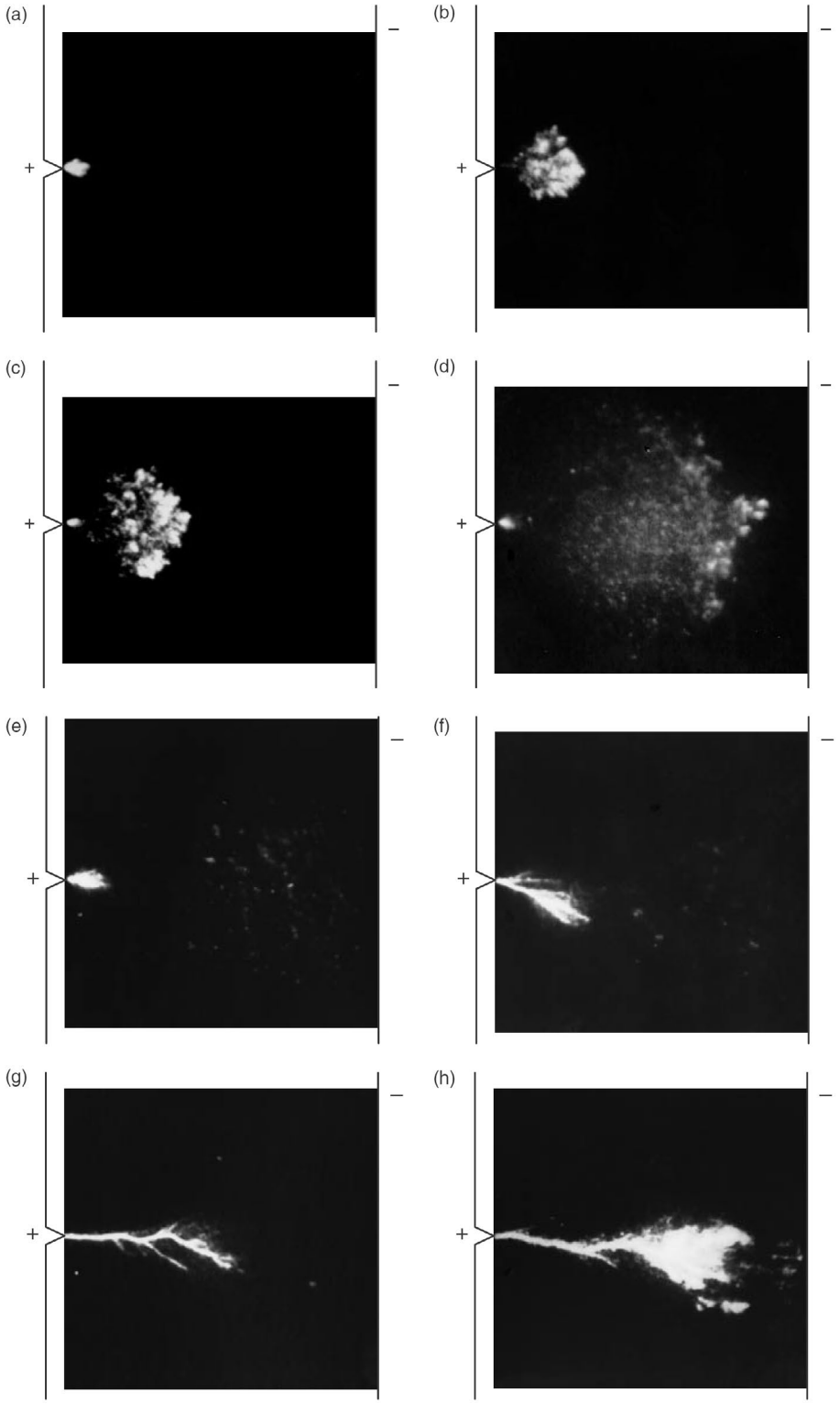


**Figure 3.** Sequence of shutter photographs of cathode-directed streamers in an atmospheric pressure, $N_2$-filled gap. The applied voltage was 98 kV. The shutter was open for 10 ns, and the photos were obtained at about (*a*) 40, (*b*) 80, (*c*) 140, (*d*) 400, (*e*) 800, (*f*) 1300, (*g*) 2100, and (*h*) 2500 ns after the applied voltage pulse.

the delay, typically from ≈1 to ≈0.2 $\mu$s. There was a similar decrease in the shot-to-shot delay jitter. The shutter photograph in figure 6(*c*) was taken with this irradiation in order to reduce the timing jitter to manageable proportions. Even with UV irradiation, the jitter in delay was similar to the time required for a streamer to traverse the gap. For this reason, we do not have good timing information for the corresponding shutter photos such as that in figure 6(*c*).

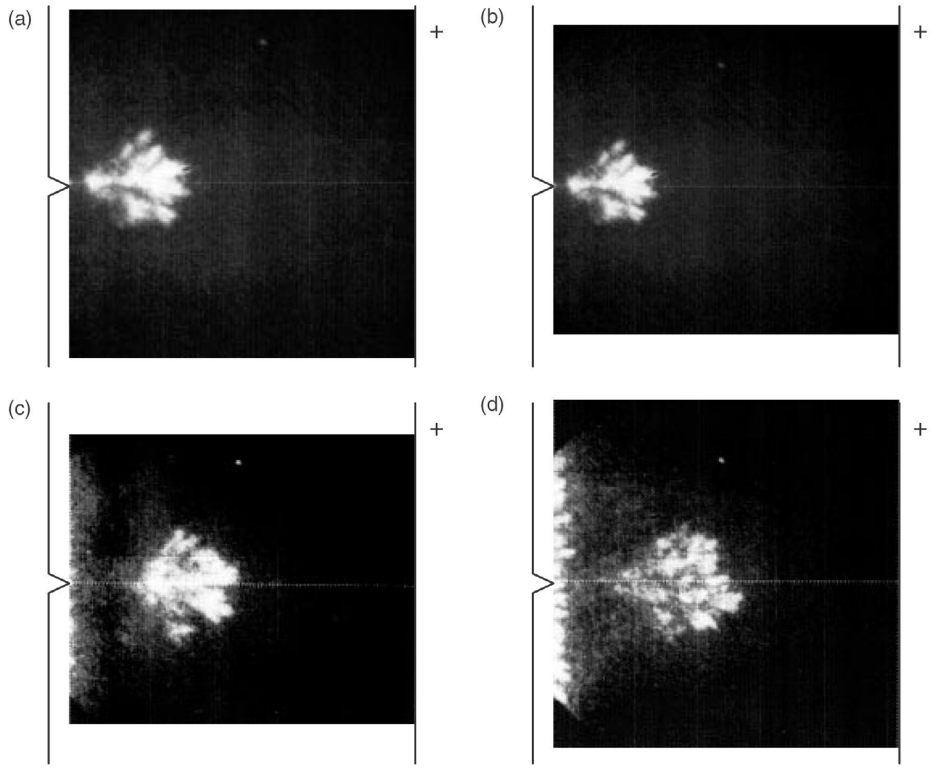


**Figure 4.** Sequence of shutter photographs of anode-directed streamers in an atmospheric pressure, $N_2$-filled gap. The applied voltage was 123 kV. The shutter was open for 10 ns, and the photos were obtained at about (*a*) 40, (*b*) 50, (*c*) 60, and (*d*) 70 ns after the applied voltage pulse. The horizontal, dotted line is an artefact introduced to aid alignment. Multiple streamers are seen in these photos emanating from the point. The features at the far left of the photos in (*c*) and (*d*) are due to streamers initiated at the rounded edge of the electrode supporting the tip.

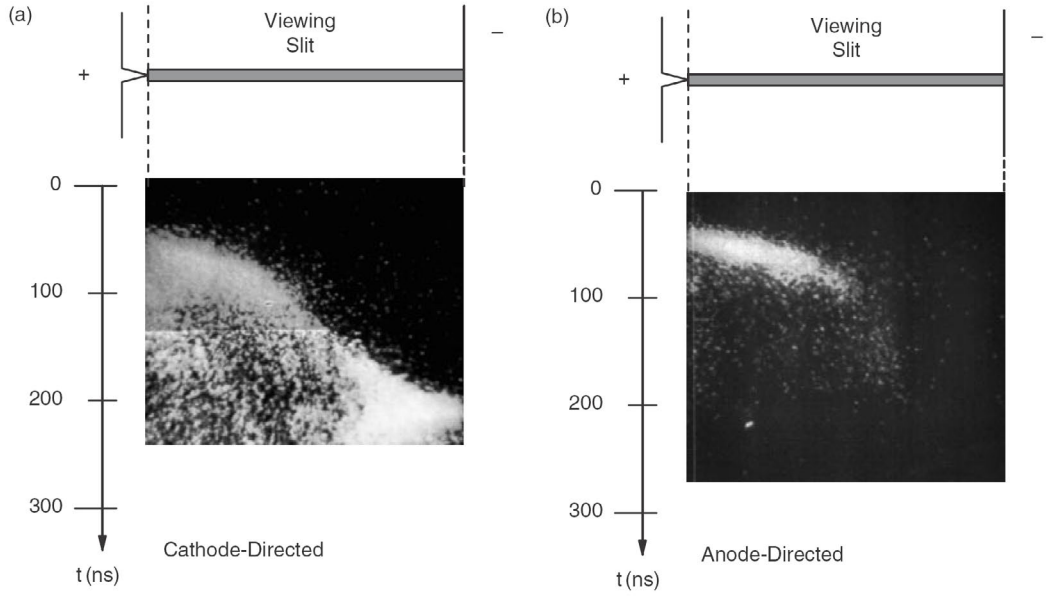


**Figure 5.** Streak photographs showing (*a*) cathode-directed and (*b*) anode-directed streamers in pure $N_2$ with charging voltage 123 kV. The sudden change in brightness in (*a*) at about 130 ns is an experimental artifact introduced by an unresolved problem in the Hamamatsu image acquisition equipment.

The addition of $O_2$ causes similar changes in the characteristics of both cathode-directed and anode-directed streamers. The number of streamers is reduced, and the apparent diameter of the streamers is increased. In the anode-directed case, the addition of $O_2$ enables streamers to traverse more of the gap. For 123 kV, 760 torr fill, and $O_2$ concentrations greater than about 1%, the streamers traversed the entire gap. Interestingly, the addition of $O_2$ did not increase significantly the initiation delay of anode-directed streamers. This behavior is consistent with the pri-

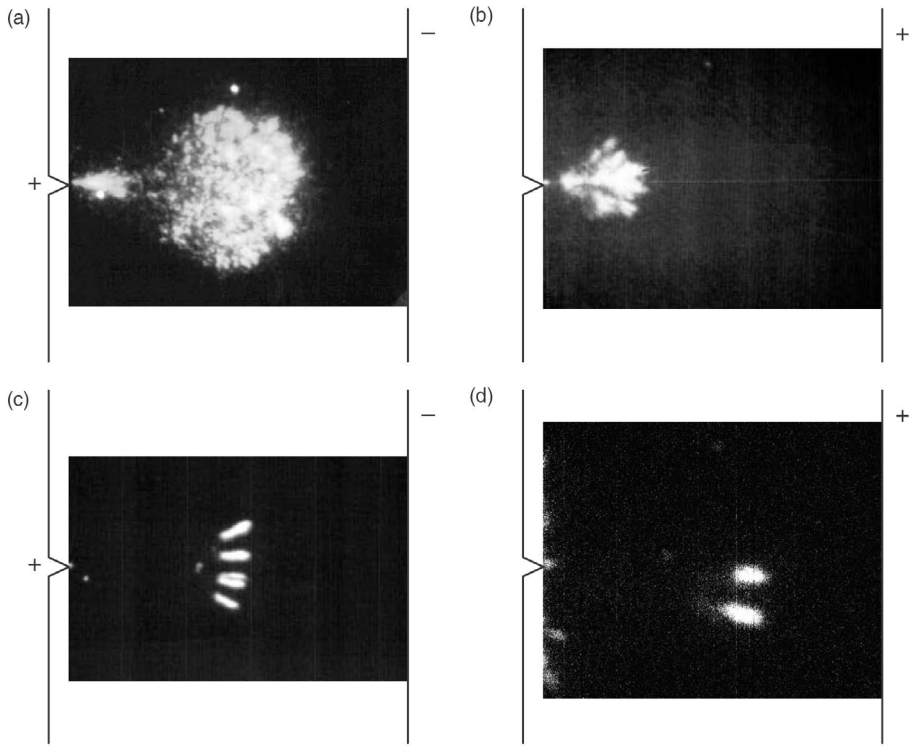


**Figure 6.** Shutter photographs showing streamers in pure $N_2$ [(*a*) and (*b*)] and mixtures containing 15% [(*c*)] and 1% [(*d*)] $O_2$. Streamers in (*a*) and (*c*) are cathode directed, those in (*b*) and (*d*) are anode directed. The features at the far left of (*b*) and (*d*) are due to streamers initiated at the edge of the charged electrode. The horizontal, dotted line in (*b*) is an artefact introduced to aid alignment.

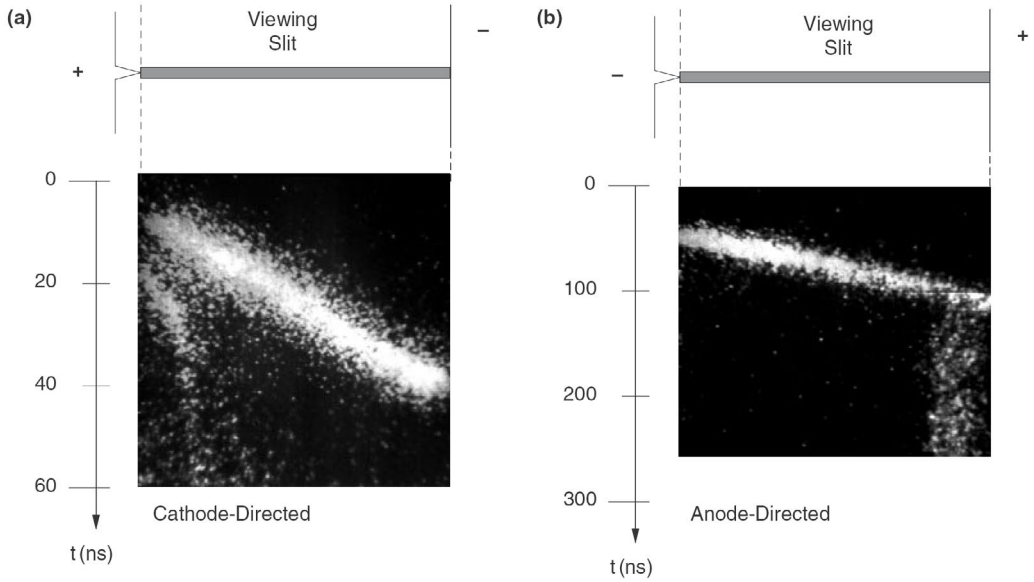


**Figure 7.** Streak photographs of streamers in $N_2/O_2$ mixtures containing 10% $O_2$. The charging voltage was 123 kV, and the pressure 760 torr. The time zero in (a) is displaced by about 1$\mu$s. In (*a*) the zero of time is displaced by about 1$\mu$s. Note the timescale difference in (*a*) and (*b*).

mary source of initial free electrons in the anode-directed configuration being field emission from the sharp point. Figure 7 shows streak photographs of cathode-directed, (*a*), and anode-directed, (*b*), streamers in atmospheric-pressure $N_2/O_2$ mixtures containing 10% $O_2$.

We have a small amount of data on streamers in $N_2/SF_6$ mixtures. These data show the same trend as the $N_2/O_2$ mixture, i.e. fewer and fatter streamers with the addition of $SF_6$. However, interpretation of the data is made difficult by the dissociation of $SF_6$ and subsequent reactions of the fragments.

### *3.2. Data compilations*

We have compiled data on streamer velocity as a function of average applied field, polarity, pressure, and fill gas composition from a large number of streak photographs such

as those in figures 5 and 7. Shutter photographs show that in most cases there is a swarm of streamers, and the value obtained from the streak photographs is actually the velocity of the leading edge of the swarm. The streamer velocity typically decreases substantially as the streamer moves out of the highly enhanced field region near the tip, becoming roughly constant after several cm. In some cases the velocity increases again as the streamer nears the opposite electrode. The velocity used in the compilation was obtained from the slope of the straight-line (constant-velocity) portion of the front seen in the streak photos. For anode-directed streamers in pure $N_2$ (see e.g. figure 5(*b*)), the determination of this slope is not as well defined because of the early disappearance of the streamer.

Figure 8 shows the streamer velocity as a function of applied voltage for pure $N_2$ and mixtures containing $N_2$ for both voltage polarities. The total pressure was 760 torr in all cases. Each data point represents four to six measurements. The central point is the average of the measured values, and the error bars give the deviations of the extreme values from the average. From these data, it is clear that the addition of $O_2$ increases streamer velocity under otherwise similar conditions. Figure 9 shows the same data but with the velocity plotted as a function of $O_2$ concentration for several applied voltages. Note the presence of zero on an apparently logarithmic horizontal scale in order that the pure $N_2$ value could be displayed. The velocity of cathode-directed streamers increases by about a factor of 2 or more with the addition of 0.1% $O_2$, but saturates with the further addition of $O_2$. Less variation with $O_2$ concentration is observed for anode-directed streamers.

The variation of streamer velocity with pressure is also of interest. Experiments were conducted in which the charging voltage was fixed, and streamer velocity measured for pure $N_2$ pressures ranging between 100 and 700 torr. These data are shown, plotted versus $E/P$, in figure 10 for streamers of both polarities. The voltage for both polarities was 98 kV. As in figures 8 and 9, each plotted point is the average of four to six values and the error bars indicate the extreme range of values found.

All of these data were taken with a fixed voltage, and a variable pressure. They do not indicate whether or not the streamer velocity is in fact a function of $E/P$. To shed some light on this question, we carried out a small set of experiments in which the voltage and pressure were varied simultaneously to maintain a constant value of $E/P$. The po-

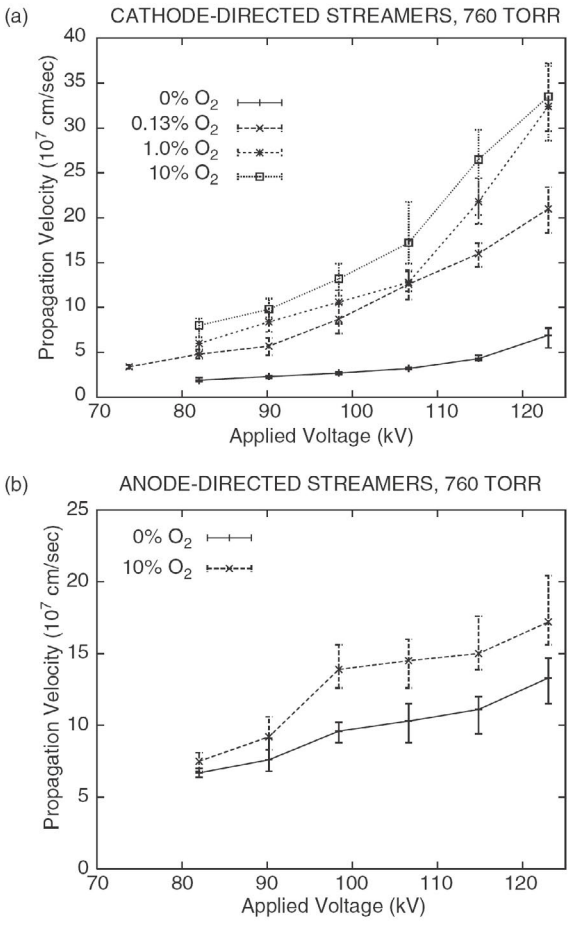


**Figure 8.** Graphs of propagation velocity versus applied voltage for (*a*) cathode-directed, and (*b*) anode-directed streamers in pure $N_2$ and mixtures containing $O_2$. The pressure was 760 torr. Each point represents the average and the error bars represent the extremes of four to six measurements. Because of the limited propagation distance of anode-directed streamers in pure $N_2$, the velocity measurements in (*b*) are somewhat subjective.

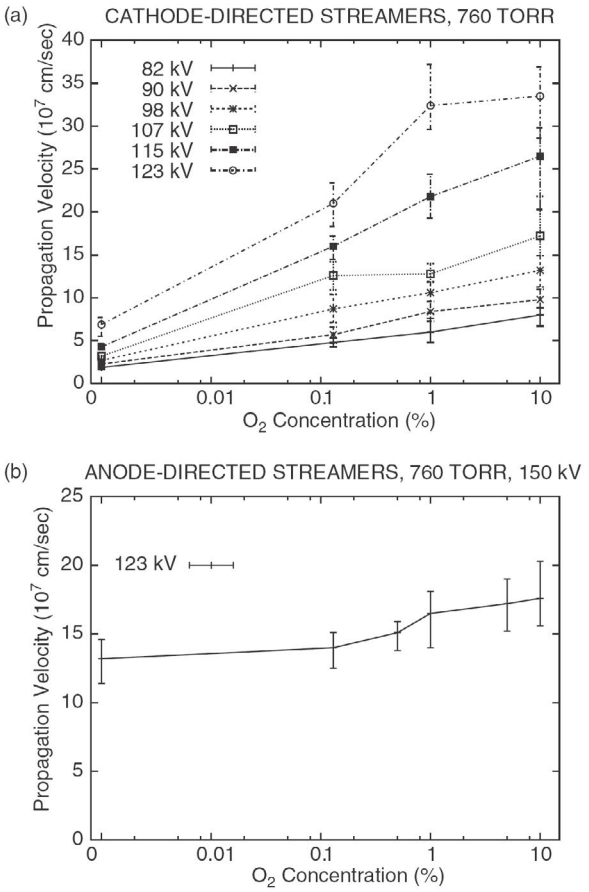


**Figure 9.** Graphs of streamer propagation velocity versus $O_2$ concentration for (*a*) cathode-directed, and (*b*) anode-directed streamers at fixed charging voltages. In (*a*) values for several charging voltages are plotted. Because of the weaker dependence of velocity on voltage and limited propagation distance of anode-directed streamers, only values for 123 kV are presented. Note that in order to plot the pure $N_2$ data, the horizontal scale is not strictly logarithmic. Each point represents the average and the error bars represent the extremes of four to six measurements.

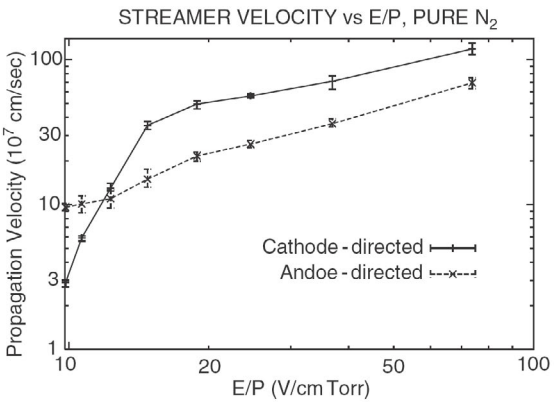


**Figure 10.** Graph showing the dependence of streamer velocity on $E/P$. Each point represents the average and the error bars represent the extremes of four to six measurements. The voltage in all cases was 98 kV, and $E$ is the average field.

larity was such as to produce cathode-directed streamers. The range of fields was limited to a variation of about a factor of 2. Over this range, for a fixed value of $E/P = 13$ V cm$^{-1}$ torr$^{-1}$ the measured velocity was constant to within about 20%, which is about the same as the shot-to-shot variation in velocities we found. We do not have similar data for anode-directed streamers.

We found that anode-directed streamers in pure $N_2$ fill gas traveled across only part of the gap, disappearing typically somewhere in midgap. This propagation distance could be measured from streak photographs such as those in figure 5(*b*). Figure 11(*a*) shows a compilation of the propagation distance in an $N_2/O_2$ mixture containing 10% $O_2$ versus charging voltage, and figure 11(*b*) shows a similar compilation at a fixed 123 kV voltage as a function of $O_2$ concentration. All data were obtained at 760 torr total pressure. At each voltage and $O_2$ concentration four to six measurements were made, and each point is plotted. The lines connect the averages.

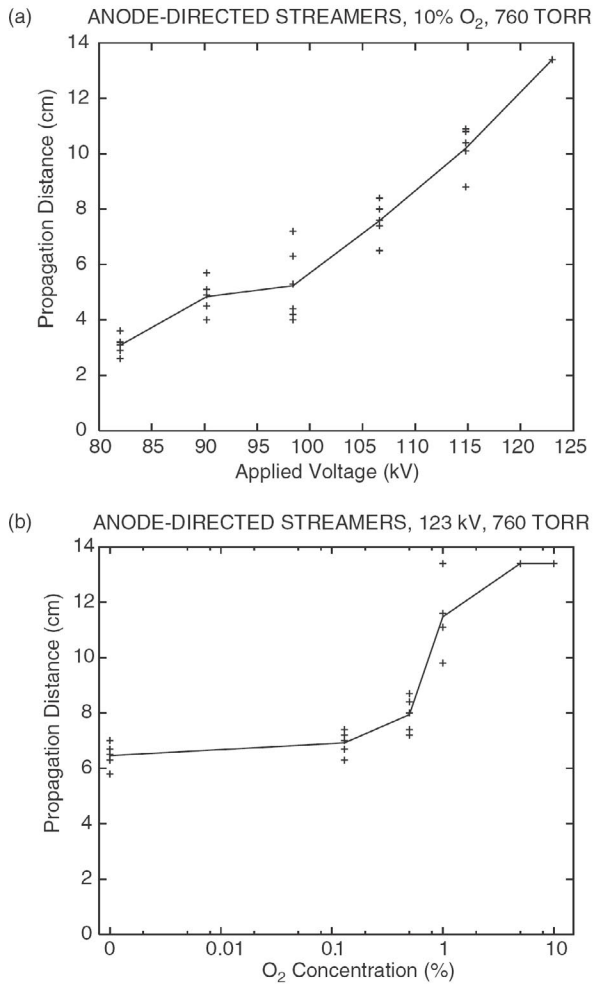


**Figure 11.** Graphs showing the dependence of the maximum propagation distance of anode-directed streamers on (*a*) voltage, and (*b*) $O_2$ concentration. In (*a*) the fill gas contained 10% $O_2$, and in (*b*) the voltage was 123 kV. The gap length was 13.4 cm. Note that in (*b*) the horizontal scale is not strictly logarithmic in order that the pure $N_2$ data could be displayed.

## 4. Discussion

Several researchers have reported empirical studies of streamer behavior under a variety of conditions. Most of these experiments were carried out in overvolted gaps, with both cathode-directed and anode-directed streamers being initiated from an electron avalanche. Until one streamer bridges the gap, the base of both streamers is connected to the cathode through a very resistive path provided by whatever free electron density is left behind in the avalanche process. Typically, the anode-directed streamer struck the anode before the cathode-directed streamer had grown appreciably. The cathode-directed streamer then propagated back toward the cathode through the detritus left behind by the electron avalanche. Our experiments differ from these in that the streamers are initiated very close to a short point projecting outwards from one electrode. This configuration has the advantage that the properties of the streamers under study are better decoupled from other events in the gap. As discussed below, several reports of streamer velocities using the constant-field configuration have appeared. Many of these results are inconsistent. At least in part, this inconsistency is probably due to the uncontrolled properties of the initiating electron avalanche. In our configuration, streamers of both polarities propagate through unperturbed gas, and the connection to one electrode is through a very short length of ionization. Thus, our results should be more reproducible and more representative of the intrinsic streamer properties than are those obtained in the more conventional configuration.

Our configuration has the further advantage that it allows us to study streamer evolution with average applied fields well below the uniform-field breakdown voltage. The main disadvantage of the configuration is the non-uniform field in the vicinity of the point which complicates data interpretation. To minimize field variation in the gap while still producing the large fields near the point required for streamer initiation, we used a flat, parallel-plane electrode configuration to define the base field in the gap, and a short (1 cm), thin (3 mm diameter), sharply pointed rod extending outward from the centre of one plane electrode to provide the high-field region needed for streamer initiation. A second disadvantage is the small ambiguity in the applied field during streamer evolution introduced by the ringing of the applied voltage pulse.

Another difference between our experiments and most previous work is the relatively long ≈13 cm gap, coupled with the use of a controlled atmosphere, good diagnostic sensitivity, and fast response time. The gap was long enough that the streamers could attain a quasi-steady-state propagation. Most previous experiments carried out in a controlled atmosphere involved a 1–3 cm gap length [3–11]. It is not clear that the streamers observed in these experiments had reached steady state, and it is therefore possible that the gap length influenced the measured properties. Exceptions include experiments by Möstl and Timm [12] and Timm [13] in a 11 cm gap, and Dawson [14] in a 5 or 7 cm gap. Experiments in gaps of several metres length have also been reported, but they were carried out in laboratory air, typically in an unshielded configuration [15]. In these experiments, it was necessary to place the optical diagnostics several metres from the breakdown path, reducing the sensitivity and spatial resolution. Also the open geometry and other factors led to relatively slow voltage risetimes. In the previous section, we presented compilations of our empirical data obtained from a large number of experiments showing streamer behavior in $N_2$ and $N_2/O_2$ mixtures. These results are generally similar to results reported by other workers, but extend substantially the information on streamer behavior. Many of the differences between results of different groups probably are due to the different experimental configurations and different regions of parameter space covered.

There have been a number of numerical calculations of streamer properties in $N_2$ and other gases [16–21]. Comparison of our results with these calculations is difficult for two reasons. First, the gap lengths are incompatible. These calculations deal with gap lengths of the order of 1 cm. Our experiments use a 13 cm gap and show that the streamer reaches a quasi-steady state only after several cm. Second, the electric field strengths are incompatible. Calculations typically use fields of 30 kV $cm^{-1}$ or larger. The average field in our experiments was 6–10 kV $cm^{-1}$. Because of these issues, we have not attempted other than general comparisons with numerical results.

### *4.1. Streamer velocity*

*4.1.1. Background.* There have been a number of reports of empirical measurements of streamer velocities and other properties. Although these papers report velocities around 108 cm $s^{-1}$, values under similar conditions differ by up to an order of magnitude.

Reported experiments generally fall into two groups. In most of the studies, streamers were initiated from an electron avalanche in an overvolted gap. The growth of ionization in the avalanche led to shielding charges and the formation of streamers, typically from some root point in midgap. Streamers propagated from the root point in both directions. Complex and not very reproducible behavior has been reported in these cases. The evolution of each streamer depends on the potential of the root point, on the conditions left by the electron avalanche, and on the propagation of the other streamer heading in the opposite direction. In experiments in the second group, streamers are initiated from a point very close to one electrode. In these experiments, streamers of a single polarity are involved, the potential of the root point is well defined, and the streamers propagate into a relatively well-defined environment. The work reported here falls into this group.

In the first group, probably the most complete study of streamer velocities was described by Wagner [3, 22]. He reports rather complex behavior, with several stages of evolution. For $E/P$ = 55 V $cm^{-1}$ $torr^{-1}$ in pure $N_2$, Wagner reports about $4 \times 10^7$ and $1 \times 10^7$ cm $s^{-1}$ for the velocities of anode-directed and cathode-directed streamers, respectively, while we find velocities more than an order of magnitude larger than he reports. Comparison of his data with ours is difficult because of the different conditions, even at similar values of $E/P$.

Bayle *et al* [23] report results from experiments similar to Wagner's. For $N_2$ they report data only for anode-directed streamers, finding velocities between 2 and $4 \times 10^8$ cm $s^{-1}$, for values of$E/P$ ranging between 155 and 185 V $cm^{-1}$ $torr^{-1}$. Chalmers *et al* [4] also report similar data, finding velocities for anode-directed streamers between about 1 and $6 \times 10^7$ cm $s^{-1}$ for $E/P$ values between 45 and 55 V $cm^{-1}$ $torr^{-1}$. These values are similar to those reported by Wagner. Stritzke *et al* [6] have published the results of a substantial study of streamer-initiated discharges in $N_2$. The conditions were similar to Wagner's. For a value of $E/P$ = 50 V $cm^{-1}$ $torr^{-1}$, they report velocities for anode-directed and cathode-directed streamers of about $5 \times 10^7$ and $7 \times 10^7$ cm $s^{-1}$, respectively. The velocity of the anode-directed streamer is similar to that found by Wagner, but that of the cathode-directed streamer is larger by a factor of 7.

For $E/P$ = 50 V $cm^{-1}$ $torr^{-1}$, we find velocities for anode-directed and cathode-directed streamers of $5 \times 10^8$ and $9 \times 10^8$ cm $s^{-1}$, respectively. In experiments such as Wagner's, streamers were initiated from an electron avalanche in an overvolted constant-field gap. Because of the poor electrical connection to the cathode, we would expect the field at the tip of the propagating streamers to be smaller in Wagner's configuration than in ours, so the difference in velocities is not surprising.

In experiments falling into the second group, Sigmond [9] reports streak photographic observations of cathode-directed streamers in air-filled, point-plane gaps of length 0.5 and 1.0 cm. Values of $E/P$ were about 12 V $cm^{-1}$ $torr^{-1}$. He found that streamer velocities increased with distance from the point, attaining about $1 \times 10^8$ cm $s^{-1}$ at the plane cathode. At a similar value of $E/P$ in a 90/10% $N_2/O_2$ mixture we find about $1.4 \times 10^8$ cm $s^{-1}$.

Dougal and Williams [10] report observation of a streamer in an $N_2$-filled, laser-triggered, 0.5 cm spark gap. The conditions in this study are similar to those in this paper in that the streamer is initiated from the surface of one electrode of a nearly constant-field gap. Besides the much shorter gap length, they differ in that the streamer is initiated from a small plasma fireball produced by the focused output beam of an Nd:YAG laser, and that the laser beam interacted with the propagating streamer. For $E/P$ = 42 V $cm^{-1}$ $torr^{-1}$, they found a velocity of about $2 \times 10^8$ cm $s^{-1}$. This value is about a factor of 3 slower than we observe at the same value of $E/P$.

Peterkin and Williams [24] report the observation of streamers in an $N_2$-filled trigatron spark gap. They report

the transit time for a 2.5 cm gap as a function of applied voltage and polarity. At 700 torr pressure, they find similar transit times for streamers of both polarities. These translate to average propagation velocities ranging from about 1.7–3.6 × $10^8$ cm $s^{-1}$ for values of $E/P$ ranging from 26–34 V $cm^{-1}$ $torr^{-1}$. For anode-directed streamers, these values are similar to those we find in this paper. For cathode-directed streamers, these values are about half what we find here. Comparison of the two data sets is complicated by the effects of the trigger electrode in the trigatron configuration.

*4.1.2. Variation with $O_2$ addition.* We find that the addition of $O_2$ to $N_2$ increases streamer velocities under otherwise similar conditions. The effect is particularly marked for the case of cathode-directed streamers. $O_2$ differs from $N_2$ in two important respects. First, $O_2$ is a low-energy electron attacher, whereas $N_2$ is non-attaching. On this basis, one would expect the addition of $O_2$ to hinder, rather than aid, streamer propagation. The second difference is that the range of the photoionization process is considerably longer for $O_2$ than $N_2$. Penney and Hummert [25] have measured the photoionization properties of $N_2$, $O_2$, and air. They find that at 760 torr, for example, and a fixed electron impact ionization rate the photoionization rate in $O_2$ is about 20 times that in pure $O_2$, at a range of 0.07 cm. Since streamer propagation is strongly dependent on the photoionization process, we conclude that the increase in velocity on addition of $O_2$ is due to the effect of $O_2$ on the photoionization characteristics of the fill gas ahead of the streamer.

This conclusion is supported by our data on the polarity dependence of streamer velocities. Photoionization plays a more important role in streamer propagation for cathode-directed streamers than for anode-directed streamers. Thus, one would expect the addition of $O_2$ to affect streamer velocity more strongly for cathode-directed than for anode-directed streamers. This effect is observed experimentally. At 98 kV charging voltage, the addition of 10% $O_2$ increases the velocity of cathode-directed and anode-directed streamers by factors of about 4 and 1.4, respectively.

### 4.2. Streamer morphology

*4.2.1. Streamer diameter.* The optical emission observed in shutter photographs results from electron impact excitation of fill gas molecules. The width of the streamer tip images in the direction perpendicular to travel is thus a measure of the streamer diameter. For cathode-directed streamers in pure $N_2$, such as shown in figure 3, it is difficult to measure this diameter accurately because of spatial resolution limitations, but it is about 2mm or less. Images of anode-directed streamers under similar conditions are more diffuse, and the boundaries are more poorly defined. In the photographs in figure 4, the apparent diameter is about 4 mm. The addition of $O_2$ increases the diameter of streamers of both polarities. With 10% $O_2$, the diameter of cathode-directed and anode-directed streamers are about 6 and 8 mm, respectively.

The field direction for anode-directed streamers is such as to pull free electrons outward from the streamer tip, whereas for cathode-directed streamers it pulls electrons inward, tending to concentrate them. Thus, the larger, more diffuse structure of anode-directed streamers is expected. The observed increase in streamer diameter upon addition of $O_2$ is consistent with the important role played by photoionization, as deduced from the streamer velocity data. The increased photoionization range in $O_2$-containing mixtures would have two effects. First, it would tend to place seed electrons farther away from the region of maximum field, thus broadening the streamer. Second, it would reduce the field enhancement needed to allow streamer propagation at a given rate, thus allowing streamers with blunter, more rounded tips to propagate.

*4.2.2. Streamer branching.* Our data provide clear and convincing evidence that streamers in atmospheric pressure, pure $N_2$ branch frequently. Although accurate quantitative data is difficult to extract, the average branching distance for the cathode-directed streamers in figure 3, for example, is about 3 mm. For anode-directed streamers, the mean branching distance is somewhat longer, about 1 cm. This degree of branching is unexpected, and to our knowledge has not been reported previously. The addition of small amounts of $O_2$ sharply reduces the branching.

The physical reason for the high branching frequency of streamers in pure $N_2$ and the decreased frequency in $N_2/O_2$ mixtures is probably related to the photoionization properties of the fill gas. In the case of pure $N_2$, a narrow, sharp, streamer tip is needed to provide adequate field enhancement for propagation because of the short photoionization range. In this case broadening forces lead to bifurcation, rather than increased diameter. For $O_2$-containing mixtures, the increased photoionization range allows streamers with smaller field enhancement to propagate, and streamers can broaden without bifurcation.

*4.2.3. Streamer robustness.* We also find that anode-directed streamers are not as robust as cathode-directed streamers under similar conditions. At the highest voltage we investigated (123 kV, corresponding to an average $E/P$ of about 12 V $cm^{-1}$ $torr^{-1}$), anode-directed streamers propagated only about 6 cm in a 13 cm gap filled with pure, atmospheric pressure $N_2$. In contrast, the cathode-directed streamers always crossed the gap, even at 80 kV ($E/P$ = 8 V $cm^{-1}$ $torr^{-1}$). Further, the optical emission from cathode-directed streamers was more intense than that from anode-directed streamers under similar conditions, suggesting that the electric field at the streamer tip was larger in the cathode-directed case. Higher fields are generally observed in cathode-directed streamers in numerical simulations [16], and our results support these simulations in this aspect. Apparently, the outward drift of free electrons from the anode-directed streamer tip tends to spread out the shielding charge at the tip, decreasing the field enhancement. Electron impact ionization then decreases as well, reducing further the charge density available for shielding, and causing the streamer to decay into an electron cloud drifting in a field insufficient to produce significant impact ionization or even excitation.

As an aside, the decreased range of anode-directed streamers in air is tacitly recognized by standard engineering practice for high-voltage DC power transmission lines. In a unipolar system, the power line is designed to have

negative polarity with respect to ground in order to reduce corona and associated RF interference [26].

Figure 11(*a*) shows that the dependence of the propagation distance of anode-directed streamers in pure $N_2$ on applied voltage is approximately linear, with an *x*-axis intercept at about 65 kV. It does not appear that the limited propagation distance is caused by a critical field effect because the field in the middle of the gap should be nearly position independent, and there should then be a critical applied voltage, with short streamers below the threshold, and full gap propagation above it. We do not understand the increase in propagation distance with $O_2$ addition. Since we have argued that the limited propagation distance in pure $N_2$ is due to the drift of electrons away from the streamer head, it does not seem likely that a significantly increased propagation distance would result from the increased photoionization range in $O_2$-containing mixtures. Perhaps the relatively immobile negative ions are playing a role.

### *4.3. Other streamer properties*

*4.3.1. Streamer initiation delay.* There was a delay between the arrival of the voltage pulse at the spark gap and the appearance of emission associated with streamer creation near the point. Besides the finite risetime of the voltage pulse ≈20 ns, the delay may also be the result of an initial-electron effect ("statistical lag"), or of the finite time required for an initial electron to avalanche into the ≈108 electrons required for streamer initiation ("formative lag") [27, 28]. This latter process was a major source of delay in overvolted, constant-field gap experiments such as Wagner's [3, 22], but is generally insignificant in our experiments because of the high field enhancement near the point in our work.

For cathode-directed streamers in pure $N_2$, the delay ranged from 30 to 60 ns, with most delays being 30–40 ns. For anode-directed streamers the delay was about 30 ns, with little shot-to-shot variation. The 30 ns delay time for anode-directed streamers is consistent with the ≈20 ns risetime of the voltage pulse and the ≈10 ns time required for the excited state populations responsible for the visible emission to build up to the "steady-state" value.

For cathode-directed streamers the delay in excess of 30 ns appears to be primarily a result of the requirement that a free electron appear in some small, high-field, volume near the point ("statistical lag"). This conclusion is supported by the observation that the addition of $O_2$ increased the delay for cathode-directed streamers to about 1$\mu$s, with similar jitter, whereas the delay for anode-directed streamers remained about 30 ns. In this model, for the shots with ≈30 ns delay there was already a free electron in the high-field region very close to the point, whereas in shots with longer delay there was not. The addition of $O_2$ would reduce the probability that an electron would be found in the high-field region because it reduces the free-electron density.

To check on this hypothesis we roughly estimate the minimum free-electron density required to have, on the average, one electron in a region of sufficiently high field to initiate a streamer with a time insignificant on the empirical timescale (taken as 1 ns). We assume that streamer initiation occurs when the total number of free electrons in the nascent streamer head equals $10^8$, and we define the "high-field" region by requiring that a single free electron placed within the region create $10^8$ free electrons within 1 ns. Using data for the Townsend ionization coefficient and electron drift velocity in $N_2$ [2], we estimate the minimum field to be about 80 kV cm$^{-1}$. We can estimate the spatial dependence of the field near the point by approximating the point as a sphere inside a very much larger grounded sphere. The field a distance $r$ from the centre of the inner sphere is about

$$E(r) = V(r_0/r^2)$$

where $r_0$ is the inner sphere radius and $V$ is the charging voltage. Taking the inner sphere radius to be 0.01 cm, and the voltage to be 150 kV, $E$ falls to 80 kV cm$^{-1}$ at about 0.14 cm. The volume of the high-field region is then about 0.01 cm$^3$, and the minimum free-electron density required to average one electron in the front half of the sphere is about 200 cm$^{-3}$.

This value is much larger than the free-electron density predicted by the Saha equation, but is similar to values found empirically in air [29]. The discrepancy is due to non-equilibrium resulting from the long electron recombination/attachment time. The free-electron density would be larger in pure $N_2$ than in air because of the corresponding increase in recombination/attachment time.

Our statistical lag hypothesis is consistent with these estimates. The hypothesis is also supported by our observation that the delay time in $O_2$-containing mixtures was reduced substantially by irradiating the gap with light from a small Hg calibration lamp. Presumably, the light photoionizes negative $O_2$ ions, reducing the overall electron attachment rate and increasing the free-electron density.

For anode-directed streamers, the delay remained about 30 ns even with the addition of $O_2$. This constant delay is consistent with the occurrence of field emission from the point cathode. The existence of such emission even at fields below 100 kV cm$^{-1}$ has been shown by several workers [30–32].

*4.3.2. Gap current.* Capacitive voltage divider probes in the experimental cell allowed measurement of the gap current by measuring the voltage across the 50 Ω load resistor. Unfortunately, the transient electrical noise associated with firing the laser-triggered spark gap was much larger in amplitude than the signal associated with the gap current during streamer propagation. This noise lasted for about 500 ns, and was due primarily to the reflections between the open ends of the transmission line. Thus, we do not have any meaningful data on gap current for most of our experiments.

For cathode-directed streamers in $O_2$-containing mixtures, however, the delay between the arrival of the voltage pulse and streamer initiation could be as long as several $\mu$s—long enough for the electrical noise to die away. In such cases, we were able to obtain gap current information. Figure 12 shows a time-synchronized shutter photograph, (*a*), and current oscillogram, (*b*), for a mixture containing 15% $O_2$ at 760 torr.

The shutter opened at time $t = 0$ on the current trace and it was open for about 10 ns. The $t = 0$ time is about 2$\mu$s after the voltage pulse arrived at the gap. It appears the streamers were initiated at about $t = -80$ ns, and the shutter photograph shows that the lead streamer had nearly

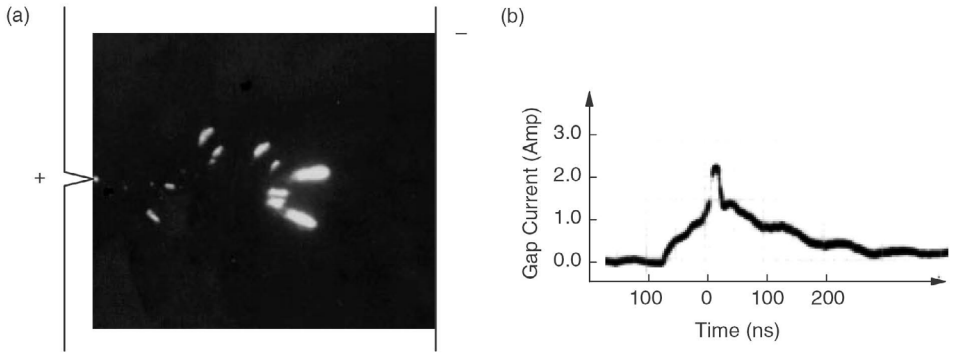


**Figure 12.** Time-synchronized shutter photograph, (*a*), and current trace, (*b*), obtained from several cathode-directed streamers traversing the gap in a 760 torr $N_2/O_2$ mixture containing about 15% $O_2$. The voltage was 98 kV, giving $E/P = 10\text{Vcm}^{-1}\text{ torr}^{-1}$. The $t = 0$ time on the current trace occurred about 2 $\mu$s after the application of voltage to the gap, and corresponds to the time when the shutter photograph was taken.

traversed the gap at $t = 0$. These data are consistent with streak photographs such as that in figure 7, which show a similar transit time. After an initial jump coincident with streamer initiation, the current rises approximately linearly until the time when the first streamer strikes the cathode, whereupon a small current pulse of magnitude about 1A and duration 15 ns occurs. The current before this pulse is due to displacement current from the positively charged streamer heads moving toward the cathode at $10^8$ cm $s^{-1}$. The origin of the current pulse is less clear. It should not be the result of neutralization of the free positive charge at the streamer head because the displacement current should have already accounted for this. The pulse is probably due to a redistribution of free charge inside the streamer body. Similar features were seen in most data taken under these conditions, and a similar feature has also been seen in trigatron gaps [24].

The unshielded positive charge in the streamer heads can be estimated from the current data obtained before the gap is bridged. For infinite plane-parallel electrodes, the displacement current resulting from a charge $q$ travelling at constant velocity $v$ would be $I = qv$. Using the known streamer velocity of $10^8$ cm $s^{-1}$, and the measured current of 1A, the charge is $10^{-8}$ C = $6 \times 10^{10} q_e$. There are several streamers in transit, so the charge in the lead streamer is some fraction of this value, perhaps $1 \times 10^{10} q_e$.

The current measurement also provides information about the average electron density in the body of the streamer. Just after the lead streamer strikes the cathode, the full gap voltage is applied across the channel, and the corresponding current value can be used to obtain an average density in the channel. Approximating the electric field as a constant 9 kV $cm^{-1}$ in the channel, and using a cross-sectional area of 0.7 $cm^2$ obtained from the shutter photographs, we estimate the free-electron density in the streamer body to be $6 \times 10^{13}$ $cm^{-3}$. The assumptions of a uniform field distribution and constant electron density with the streamer body are certainly not accurate. Also, several streamers are propagating in the gap, so the observed current should have been divided in some way between them. Nevertheless, this procedure provides a reasonably direct measure of the magnitude of the free-electron density within the streamer body.

These data also allow an estimate of the thickness of the charge sheath at the streamer tip. Approximating the sheath as a disk of thickness $\Delta x$, and cross-sectional area 0.7 $cm^2$, assuming a positive ion density in the streamer body of $6 \times 10^{13}$ $cm^{-3}$, and requiring a total sheath charge of $6 \times 10^{10} q_e$, as estimated above, yields a sheath thickness of $\Delta x \approx 14$ $\mu$m.

### *4.4. The heating phase*

After the streamers have crossed the gap, the electrodes are bridged by a region of tenuous and inhomogeneous ionization density. Because of the low ionization density and of the inhomogeneities, the bridge has a high resistance. In figure 12, for example, less than 1A of current flows during a time when nearly the full 98 kV charging voltage is applied to the gap, making the effective resistance of the gap more than 100 kΩ. The free-ionization density increases with time, probably due to heating, decreasing the effective resistance of the channel until current is limited by the 100 Ω generator resistance, rather than the gap resistance. The timescale for this transition is about 10 $\mu$s. We were primarily interested in the first phase of breakdown, involving the propagation of streamers across the virgin gap, but we also obtained data during this second phase. There have been many reports of studies of this second stage of breakdown [33]. Perhaps the most complete such study was performed over a period of several years by a group at *Les Renardieres* using non-uniform-field gaps of 3–10 m length [34].

Figures 3(*d*)–(*h*) show a sequence of shutter photographs of our gap during this phase. The first, figure 3(*d*), was acquired about 400 ns after the first streamers had crossed the gap. Besides a multi-filamentary structure emanating from the point, there are several small, apparently isolated, regions of emission. This emission marks high-field regions within the inhomogeneous ionization left by the streamers. With time, these isolated emission regions become less prominent and the multi-filamentary structure lengthens. When this structure reaches the opposite electrode, gap resistance falls rapidly and the voltage across the gap collapses, signalling full breakdown.

Figure 13 shows a montage of the breakdown process in our gap made from a number of shutter photographs. The timescale is approximately logarithmic, and the camera sensitivity decreases substantially with time, so that the emission intensity is much higher in the later stages than in the earlier. Streamers propagate across the gap during

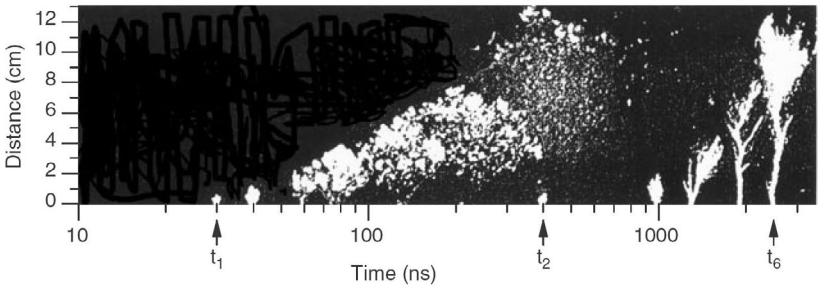


**Figure 13.** Typical sequence of shutter photographs of the cathode-directed streamer in point-plane gap, and fill gas pure $N_2$, at atmospheric pressure. The shutter was open for 10 ns. The point extended 0.9 cm into the gap, the distance from the tip of the point to the opposite electrode was 13.4 cm. The voltage was 98 kV with 20 ns risetime. (From Dale, fig 5.39 in [33].)

the first 400 ns, labelled $t_2$ in the figure. After this point, the ionization in the gap evolves, with a bright, multi-filamentary structure slowly growing outward from the point electrode. After about 1 $\mu$s, this structure becomes better defined, and propagates across the gap in a path containing a series of branches. During this time, gap current is slowly increasing. At some time, labelled $t_6$ in the figure, the structure contacts the opposite electrode. Shortly thereafter, gap current rises rapidly, and the gap voltage collapses.

In spite of the differences between the long-gap experiments and ours, streak and shutter photographs of this second phase of breakdown process are similar [33, 34]. Dale has obtained an unpublished sequence of shutter photographs from a 1.75 m gap [33] which are remarkably similar to the montage of photos shown in figure 13.

In long-gap breakdown, "restrikes" sometimes occur shortly after the streamers have traversed the gap. These phenomena are manifested by a backward-travelling wave of luminosity travelling from the planar electrode to the tip of the nascent leader. Although not evident in figure 13, we also see such phenomena, and attribute them to a redistribution of the electric field within the gap resulting from the establishment of a resistive connection between the two gap electrodes.

In both our experiments and in those with much longer gaps the bright structure grows outward from the pointed electrode. In long gaps, this structure is termed a *leader*. In our gap the propagation of the structure was rather erratic, with considerable variation from shot-to-shot, but propagation velocities were typically in the range of 5–10 × $10^6$ cm $s^{-1}$. Similar propagation velocities are seen for leaders in long gaps. It is likely, then, that the growing structure we see is due to the same physical processes as the long-gap leader, and it should be possible to study this phase of long-gap breakdown in a more controlled environment than a 5 m open gap.

## 5. Summary

We have presented a large volume of experimental data on streamer behavior in point-to-plane gaps. Our results provide more extensive coverage of streamer behavior for *E/P* values below about 50 V $cm^{-1}$ $torr^{-1}$ than has been available previously. Besides allowing us to study streamers at *E/P* values well below that required for a uniform-field breakdown, our 13 cm point-plane gap also allows direct interpretation of the data to yield understanding of intrinsic streamer behavior.

Our results suggest strongly that the photoionization process plays an important role in determining streamer evolution. In particular, the range of the photoionization process seems to be important in determining the geometry and size of the streamer tip, thereby influencing streamer evolution. It would be instructive to simulate in a numerical model the effects of different photoionization characteristics on streamer evolution for comparison with our data showing the behavior upon addition of $O_2$ to $N_2$.

**Acknowledgments**
This work was supported by the Electric Power Research Institute and the Nebraska Energy Office.

## References

[1] Bazelyan E M and Raizer Y P 1997 *Spark Discharge* (Boca Raton: CRC Press)

[2] Dutton J 1975 A survey of electron swarm data *J. Phys. Chem. Ref. Data* **4** 577-856

[3] Wagner K H 1966 Die entwicklung der elektronenlawine in den plasmakanal, untersucht mit bildverstarker und wischversluss *Z. Phys.* **189** 465-515

[4] Chalmers L D, Duffy H and Tedford D J 1972 The mechanism of spark breakdown in nitrogen, oxygen, and sulphur hexafluoride *Proc. R. Soc. Lond.* A **329** 171

[5] Giesselmann M, Pfeiffer W and Wolf J 1987 Short time optical and electrical diagnostics of pulsed $N_2$ and $SF_6$ discharges *Proc. 6th IEEE Pulsed Power Conf.* ed B H Bernstein and P J Turchi (New York: IEEE) 182-6

[6] Stritzke P, Sander I and Raether H 1977 Spatial and temporal spectroscopy of a streamer discharge in nitrogen *J. Phys.* D **10** 2285

[7] Marode E 1975 The mechanism of spark breakdown in air at atmospheric pressure between a positive point and a plane. I. Experimental: nature of the streamer track *J. Appl. Phys.* **46** 2005

[8] Byszewski W W, Enright M J and Proud J M 1982 Transient development of nanosecond gas discharges *IEEE Trans. Plasma Sci.* **10** 281-5

[9] Sigmond R S 1984 The residual streamer channel: return strokes and secondary streamers *J. Appl. Phys.* **56** 1355-70

[10] Dougal R A and Williams P F 1984 Fundamental processes in laser-triggered electrical breakdown of gases *J. Phys. D: Appl. Phys.* **17** 903

[11] Peterkin F E and Williams P F 1988 The physical mechanism of triggering in trigatron spark gaps *Appl. Phys. Lett.* **53** 182

[12] Möstl K and Timm U 1968 Zum entladungsaufbau der spuren in funkenkammern (On the discharge mechanism in spark track chambers) *Z. Phys.* **209** 60

[13] Timm U J 1973 The development of single streamers started by laser light at high overvoltages in rare gases *J. Phys.* D **6** 1891

[14] Dawson G A 1965 The lifetime of positive streamers in a pulsed point-to-plane gap in atmospheric air *Z. Phys.* **183** 172

[15] Gallimberti I 1979 The mechanism of the long spark formation *J. de Physique* **40** C7-193

[16] Dhali S K and Williams P F 1987 Two-dimensional studies of streamers in gases *J. Appl. Phys.* **62** 4696-707

[17] Wu C and Kunhardt E E 1988 Formation and propagation of streamers in $N_2$ and $N_2$ - $SF_6$ mixtures *Phys. Rev.* A **37** 4396

[18] Dhali S K and Pal A K 1988 Numerical simulation of streamers in $SF_6$ *J. Appl. Phys.* **63** 1355

[19] Morrow R and Lowke J J 1997 Streamer propagation in air *J. Phys. D: Appl. Phys.* **30** 614-27

[20] Vitello P A, Penetrante B M and Bardsley J N 1994 Simulation of negative-streamer dynamics in nitrogen *Phys. Rev.* E **49** 5574

[21] Kulikovsky A A 1994 The structure of streamers in $N_2$: II. Two-dimensional simulation *J. Phys. D: Appl. Phys.* **27** 2564-9

[22] Wagner K H 1967 Vorstadium des funkens, untersucht mit dem bildverstarker *Z. Phys.* **204** 177-97

[23] Bayle M, Bayle P and Crokaert M 1975 The development of breakdown in a homogeneous field at high overvoltages in helium - neon mixtures and nitrogen *J. Phys.* D **8** 2181

[24] Peterkin F E and Williams P F 1989 Triggering in trigatron spark gaps: a fundamental study *J. Appl. Phys.* **66** 4163

[25] Penney G W and Hummert G T 1970 Photoionization measurements in air, oxygen, and nitrogen *J. Appl. Phys.* **41** 572

[26] Kimbark E W 1971 *Direct Current Transmission* vol 1 (New York: Wiley)

[27] Raether H 1940 Zur entwicklung von kanalentladungen *Archiv für Electrotechnik* **34** 49-56

[28] Loeb L B and Meek J M 1940 The mechanism of spark discharge in air at atmospheric pressure. I *J. Appl. Phys.* **11** 438-47

[29] Morgan C G 1978 *Electrical Breakdown of Gases* ed J M Meek and J D Craggs (New York: Wiley) 655

[30] Morgan C G and Harcombe D 1953 *Proc. Phys. Soc.* B **66** 673

[31] Jones F L, de la Parrelle E T and Morgan C G 1950 Comptes Rendus **231** 514

[32] Little R P and Whitney W T 1963 Electron emission preceding electrical breakdown in vacuum *J. Appl. Phys.* **34** 2430-2

[33] Waters R T 1978 Spark breakdown in non-uniform fields *Electrical Breakdown of Gases* ed J M Meek and J D Craggs (New York: Wiley)

[34] Le groupe des Renardières 1977 Positive discharges in long air gaps at les renardieres - 1975 results and conclusions *Electra* **53** 31-153